

A CFD STUDY OF NATURAL CONVECTION HEAT AND MASS TRANSFER IN RESPIRING HYGROSCOPIC POROUS MEDIA

Mahesh PRAKASH¹, Özden F. TURAN¹, Yuguo LI² and Graham R. THORPE¹

¹Victoria University, Faculty of Engineering and Science, Victoria, AUSTRALIA

²CSIRO Division of Building Construction and Engineering, Highett, Victoria, AUSTRALIA

ABSTRACT

A model is presented to predict heat and mass transfer in a system consisting of a turbulent flow overlying a saturated hygroscopic porous medium. Comparisons with experimental and numerical simulations have been carried out to check the accuracy of components of the model. A case study using silica gel as a representative hygroscopic porous medium is simulated to illustrate an application of the model. The work is progressing towards a mathematical description of respiring agricultural products.

KEYWORDS

Hygroscopic, natural convection, porous medium, turbulence.

NOMENCLATURE

c	specific heat at constant pressure [$\text{Jkg}^{-1}\text{K}^{-1}$]
c_{e1}, c_{e2}, c_{e3}	coefficients associated with the dissipation of turbulence kinetic energy, equation (5)
C_F	Forchheimer coefficient, equation (2)
c_μ	dimensionless coefficient, equations (2a) and (11)
D	width of the system [m]
g	acceleration due to gravity [ms^{-2}]
h_p	height of porous layer [m]
h_s	heat of sorption of water [Jkg^{-1}], equation (3)
H	height of the system [m]
H_w	integral heat of wetting [Jkg^{-1}], equation (3)
k	turbulence kinetic energy [m^2s^{-2}]
K	permeability [m^2]
p	pressure [Pa]
P_{atm}	atmospheric pressure [Pa], equation (10)
Pr	Prandtl number
r	relative humidity
Sc	Schmidt number
t	time [s]
T	temperature [K]
u	fluid velocity [ms^{-1}]
u^*	friction velocity [ms^{-1}], equation (12)
w	air moisture content on dry basis, [kg of moisture/kg of dry air]
W	porous medium moisture content on dry basis, [kg of moisture/kg of dry solid]
x	space co-ordinate [m]
y	space co-ordinate or normal distance from the wall [m], equation (11)

Greek symbols

β	coefficient of thermal expansion [K^{-1}]
δ_{ij}	Kronecker delta operator
ε	dissipation of turbulence kinetic energy [m^2s^{-3}]
ϕ	porosity
μ	fluid viscosity [$\text{kgm}^{-1}\text{s}^{-1}$]
μ_t	eddy viscosity [$\text{kgm}^{-1}\text{s}^{-1}$]
ρ	density [kgm^{-3}]
σ	turbulent analogue for Prandtl and Schmidt numbers, equations (3), (4), (5) and (7)
τ	shear stress [$\text{kgm}^{-1}\text{s}^{-2}$]

Subscripts

0	reference
abs	absolute value, equation (9)
eff	effective value for porous medium
f	fluid phase (air)
i, j	direction of vector component ($i, j=1, 2$)
k	turbulence kinetic energy
m	moisture, equation (7)
s	solid phase
sat	saturation value, equation (9)
T	temperature
w	water
ε	dissipation of turbulence kinetic energy

INTRODUCTION

Experimental and numerical investigations of natural convection flows in a clear fluid overlying a saturated porous medium have been confined to studies in the laminar regime. In many practical situations, however, one encounters systems in which the heat and mass transfer is significantly affected by turbulence at least in the fluid region. Such a two layer system can be encountered in storage of porous materials such as grains, fruits and catalysts. Thermal insulation in buildings and geothermal reservoirs are also modelled as two-layer systems. In all examples mentioned above, the fluid (which is generally air), can often be turbulent. It is well established from natural convection studies in clear fluids, (the experimental study of Kirkpatrick and Bohn (1986) and numerical study of Henkes (1990)) that the enclosure dimensions determine whether the flow is laminar or turbulent. For large enclosures, the flow is turbulent due to the large Rayleigh numbers encountered. Thus, one cannot ignore turbulence as a factor which enhances heat transfer and hence moisture migration in such two layer systems, if there is a significantly large fluid layer. In the porous medium, turbulence will not persist if it has a sufficiently low permeability. Thus, one could assume a laminar regime in the porous medium.

Flow visualisations carried out with synthetic reticulated foams of different permeability values (Prakash et al. 1999a) have confirmed the validity of this assumption. This paper presents the important features of a general method of handling systems with a fluid overlying a hygroscopic porous medium where turbulence in the fluid layer is important. A detailed report of the same study has been prepared (Prakash et al., 1999c). A hygroscopic porous medium has been chosen because it is envisaged that the present model would be most useful in modelling stored agricultural products such as grains that are hygroscopic in nature. Components of the model have been validated with previous experimental and numerical results that were found to be similar to the present system. An application concerning moisture migration through a representative hygroscopic porous medium is simulated to emphasise the potential application of the model. A two dimensional system has been used in the entire paper for simplicity.

MODEL DESCRIPTION

Governing equations for fluid flow and heat transfer

Equation of continuity

$$\frac{\partial \rho_f}{\partial t} + \frac{\partial(\rho_f u_j)}{\partial x_j} = 0 \quad (1)$$

Equation of motion

$$\begin{aligned} \rho_f \frac{\partial u_i}{\partial t} + \frac{\rho_f u_j}{\phi} \frac{\partial u_i}{\partial x_j} = & -\frac{\partial p}{\partial x_i} + \frac{\partial}{\partial x_j} \left[(\mu + \mu_t) \frac{\partial u_i}{\partial x_j} \right] \\ & + \delta_{i2} \rho_f g \beta (T - T_0) \\ & - \frac{\phi \mu u_i}{K} - \rho_f \frac{C_F \phi u_i [u_j u_j]^{1/2}}{K^{1/2}} \end{aligned} \quad (2)$$

where the eddy viscosity is represented as $\mu_t = c_\mu \frac{k^2}{\varepsilon}$

$$\text{in which } c_\mu = 0.09. \quad (2a)$$

It is assumed that turbulence persists only in the fluid layer and it is rapidly attenuated in the porous medium. Thus the eddy viscosity, μ_t , applies only for the fluid layer. For the porous medium, its value is taken to be zero. The third term on the right hand side of Equation (2) is the buoyancy term which uses the Boussinesq approximation. The fourth term represents the Darcian resistance to flow. The fifth term represents the Forchheimer resistance, and it is included to account for inertial effects in the porous medium. It should be noted that the diffusion term in the momentum equation for the fluid layer becomes the Brinkman correction for the porous medium. The effective viscosity associated with the Brinkman term for the porous medium is assumed to be the

fluid viscosity. This assumption is justified due to the analysis of Neale and Nader (1974), and it has been used successfully by several authors including Singh et al. (1993), Song and Viskanta (1994) and Chen et al. (1998).

The Darcy and Forchheimer terms vanish in the fluid layer, as the fluid has infinite permeability. The porosity of the fluid layer is taken to be equal to one, and a step change in porosity and permeability is assumed at the interface between the fluid layer and porous medium.

Thermal energy balance

Due to the presence of the hygroscopic porous medium, the thermal energy balance assumes different forms for the fluid layer and the porous medium. The partial differential equations for heat, mass and momentum transfer in stored agricultural products have been derived in Thorpe et al. (1992). For the present problem one can write,

$$\begin{aligned} \left[\frac{(\rho c)_{eff}}{c_f} \right] \frac{\partial T}{\partial t} + \rho_f u_j \frac{\partial T}{\partial x_j} = & \frac{\partial}{\partial x_j} \left[\left(\frac{\mu}{Pr} + \frac{\mu_t}{\sigma_T} \right) \frac{\partial T}{\partial x_j} \right] \\ & + \frac{\rho_b h_s}{c_b} \frac{\partial W}{\partial t} \end{aligned} \quad (3)$$

where $(\rho c)_{eff} = (1 - \phi) \rho_s c_s + \phi \rho_f c_f + W c_w + \frac{\partial H_w}{\partial T}$

and $\sigma_T = 0.9$.

The term $W c_w$ arises due to the presence of moisture in the porous medium. The term H_w represents the integral heat of wetting details of which can be found in Sutherland et al. (1971). The last term on the right hand side represents the heat of sorption. It should be noted that for the fluid layer the integral heat of wetting and the heat of sorption would vanish. Again, for the porous medium the eddy viscosity term is zero, as turbulence is absent in the porous medium.

Turbulence kinetic energy balance

$$\begin{aligned} \rho_f \frac{\partial k}{\partial t} + \rho_f u_j \frac{\partial k}{\partial x_j} = & \frac{\partial}{\partial x_j} \left[\left(\mu + \frac{\mu_t}{\sigma_k} \right) \frac{\partial k}{\partial x_j} \right] \\ & + \mu_t \frac{\partial u_i}{\partial x_j} \left(\frac{\partial u_i}{\partial x_j} + \frac{\partial u_j}{\partial x_i} \right) \\ & - \beta g \frac{\mu_t}{\sigma_T} \frac{\partial T}{\partial x_2} - \rho_f \varepsilon \end{aligned} \quad (4)$$

where $\sigma_k = 1.0$

Balance for dissipation of turbulence kinetic energy

$$\begin{aligned} \rho_f \frac{\partial \varepsilon}{\partial t} + \rho_f u_j \frac{\partial \varepsilon}{\partial x_j} = & \frac{\partial}{\partial x_j} \left[\left(\mu + \frac{\mu_t}{\sigma_\varepsilon} \right) \frac{\partial \varepsilon}{\partial x_j} \right] \\ & + c_{\varepsilon 1} \frac{\varepsilon}{k} \mu_t \frac{\partial u_i}{\partial x_j} \left(\frac{\partial u_i}{\partial x_j} + \frac{\partial u_j}{\partial x_i} \right) \\ & - \rho_f c_{\varepsilon 2} \frac{\varepsilon^2}{k} - c_{\varepsilon 3} \beta g \frac{\mu_t}{\sigma_T} \frac{\partial T}{\partial x_2} \end{aligned} \quad (5)$$

where $\sigma_\varepsilon = \frac{\kappa^2}{(c_{\varepsilon 2} - c_{\varepsilon 1}) \sqrt{c_\mu}}$, $\kappa =$ von Karman's constant = 0.41, $c_{\varepsilon 1} = 1.44$, $c_{\varepsilon 2} = 1.92$.

For the coefficient $c_{\epsilon 3}$, the form suggested by Henkes (1990) is used. Thus, $c_{\epsilon 3} = \tanh|v/u|$.

It should be noted that Equations (4) and (5) apply only to the fluid layer.

Governing equations for moisture migration in porous media

Inter-granular moisture balance

The equation that governs the concentration of moisture in the air has a slightly different form in the fluid and porous layers due to the contribution of the solids to the air moisture balance in the porous medium. The air moisture balance for the porous medium can be represented by

$$\phi \rho_f \frac{\partial w}{\partial t} + \rho_f u_j \frac{\partial w}{\partial x_j} + \rho_b \frac{\partial W}{\partial t} = \rho_f \frac{\partial}{\partial x_j} \left(\frac{\mu}{Sc} \frac{\partial w}{\partial x_j} \right) \quad (6)$$

The air moisture balance for the fluid layer can be written as

$$\phi \rho_f \frac{\partial w}{\partial t} + \rho_f u_j \frac{\partial w}{\partial x_j} = \rho_f \frac{\partial}{\partial x_j} \left[\left(\frac{\mu}{Sc} + \frac{\mu_t}{\sigma_m} \right) \frac{\partial w}{\partial x_j} \right] \quad (7)$$

where, $\sigma_m = 0.65$. Note again that the eddy viscosity, μ_t , has been invoked only in the equation for the fluid layer. An order of magnitude analysis carried out on Equation (6) showed that the advection term is balanced by the change in the solids moisture content, and that the rate of change in the air moisture content is negligible in comparison. The molecular diffusion term will be significant at the interface between the porous medium and clear fluid and close to the walls. Thus, it cannot be neglected. The result enables one to neglect the first term on the left-hand side of Equation (6) thus allowing the computation of W explicitly in the porous medium. One problem encountered in a previous study by Chen et al. (1999) was with the transient computation of such systems. An implicit solution procedure was used by including all terms in Equation (6). It is expected that this problem can be overcome by using the above explicit procedure. The present formulation also allows one to take large time steps to study moisture migration once the temperature and velocity fields have evolved almost to a steady state, because the moisture field does not significantly affect the temperature and velocity fields. The ability to take large time steps during the process of computations is important due to the large time scales (days or months) encountered in such systems. Calculations are started with an initial value for moisture content of grains in the porous medium. This value is then used to calculate the moisture content of air in the porous medium. The moisture content of air in the fluid layer is calculated by using Equation (7). Silica gel is used as the representative hygroscopic porous medium for the study. Although any hygroscopic medium such as grains could be chosen, silica gel is used due to the fact that it has a linear sorption isotherm, and also because its integral heat of wetting is zero.

For silica gel,

$$W = 0.5r \quad (8)$$

where $r = p/p_{sat}$ represents relative humidity of air. The saturation pressure is given by Equation (9), (Hunter (1987)).

$$p_{sat} = \frac{6 \times 10^{25}}{T_{abs}^5} \exp\left(-\frac{6800}{T_{abs}}\right) \quad (9)$$

The moisture content of air in the porous medium is calculated by using the relationship,

$$w = \frac{0.622p}{0.622P_{atm} - p} \quad (10)$$

Problem definition, boundary and initial conditions for the case study

As a case study for the proposed model, moisture migration in a rectangular cavity of aspect ratio 2 with half the cavity filled with silica gel is chosen. A Rayleigh number, $Ra=10^{10}$ and a Darcy number, $Da = 10^{-8}$ is chosen for the study. These values correspond to a total system height, H of about 2 metres with a width, D of about 1 metre. The Darcy number chosen is typical for a storage system. Figure 1 shows a schematic diagram of the simple two-dimensional geometry considered.

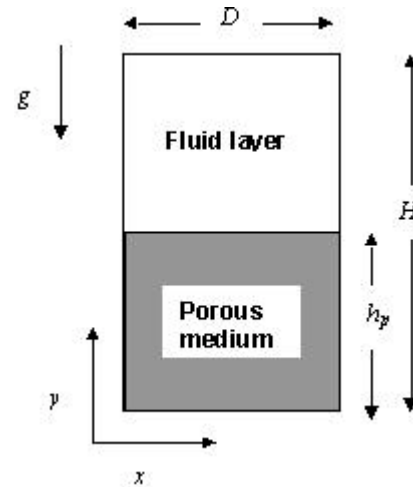


Figure 1: Schematic diagram of the system for case study.

Boundary conditions that are typical of a storage vessel are considered for the present study. The porous medium is considered to be at an elevated temperature of $T_h=30^0$ C with the side walls and the top wall at $T_c=10^0$ C. The bottom wall is considered to be adiabatic. No slip and impermeable boundary conditions are assumed for all four walls. Zero gradient boundary conditions are applied for air moisture content and moisture content of the porous medium. Hence, the system is over specified. The interface conditions for moisture and temperature are satisfied automatically as these require only a continuous change in moisture and temperature at the interface. Since the Brinkman extended Darcy flow model is implemented, the interface conditions for velocity are

also satisfied automatically through the continuity of momentum. No wall functions are used for either velocity or temperature as these are solved right up to the wall. For the turbulent kinetic energy and energy dissipation, since turbulence is assumed to be absent at the interface, conditions at the interface are taken to be identical to the wall boundary condition. Thus k and ε at the first inner grid point from the top wall, the upper portions of the lateral walls and the interface are taken as,

$$k = \frac{(u^*)^2}{\sqrt{c_\mu f_\mu}}, \quad \varepsilon = \frac{(u^*)^3}{\kappa y} \quad (11)$$

where u^* is friction velocity defined by $u^* = \sqrt{\frac{\tau_{wall}}{\rho}}$

where τ_{wall} is the wall shear stress calculated from

$$\tau_{wall} = \frac{\mu}{\rho} \left(\frac{\partial u}{\partial y} \right)_{wall}$$

the wall.

The above modification to the standard $k-\varepsilon$ model has been suggested for natural convection flows because the wall functions that normally apply for forced convection flows are not applicable for natural convection flows, see for example Henkes (1990).

Validation of the model

For the present problem, two configurations were used to validate components of the model. The simulations and experimental work of Song and Viskanta (1994) were used to validate the Brinkman Forchheimer extended Darcy flow model for a system consisting of a fluid layer adjacent to a porous layer. The turbulence model was validated with the experimental results of mixed cavity natural convection reported by Kirkpatrick and Bohn (1986) for their HCCC configuration, because the boundary conditions used closely resembled the present boundary conditions.

Method of solution

The model equations are discretised using the control volume formulation, and they are solved using the SIMPLE algorithm (Patankar, 1980). The upwind/central hybrid scheme (Patankar, 1980) is used for discretising the convection terms. The diffusion terms are discretised using the second order central scheme. The non-dimensional scheme employed by Prakash et al. (1999b) has been used for the computations. Non-uniform grid spacing was used to account for the large gradients in velocity and temperature wherever applicable. Figures 2 and 3 show schematic diagrams of the configurations of Song and Viskanta (1994) and Kirkpatrick and Bohn (1986). For the simulations of the experiments of Song and Viskanta (1994), an 80x80 grid was found to be sufficiently accurate after carrying out a grid refinement study. The streamlines and isotherms were in agreement but are not shown here.

They can be found in Prakash et al. (1999c). The comparison between the measured and simulated temperature profiles is similar to the results of Song and Viskanta (1994). This comparison is shown in Figure 4.

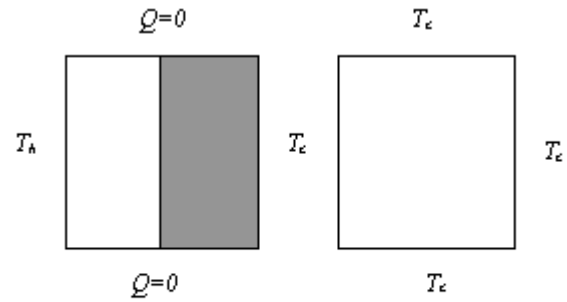


Figure 2: Schematic diagram of the configuration of Song and Viskanta (1994)

Figure 3: Schematic diagram of the configuration of Kirkpatrick and Bohn (1986)

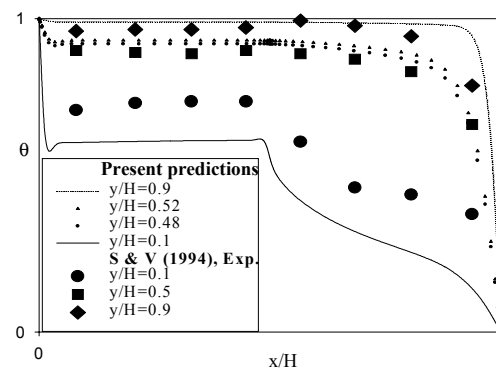


Figure 4: Temperature profiles (comparison with experiment 3 of Song and Viskanta, 1994)

The major discrepancy between the measured and predicted temperature profiles is found at $y/H=0.1$. Song and Viskanta (1994) attributed this discrepancy to the continuum model used. The modelled and experimental profiles agree in general, as pointed out by Song and Viskanta (1994). For the simulations of the experiments of Kirkpatrick and Bohn (1986) 60x60, 120x120 and 240x240 non-uniform grids were used in order to study the effect of grid refinement. For these simulations, a Rayleigh number of 10^{10} was used with the working fluid as water. All the physical properties were taken at the bulk fluid temperature. The computations were carried out until the difference between the hot wall and cold wall Nusselt numbers was less than 4%. The difference between the Nusselt numbers of the vertical walls was less than 1%. It can be seen that with a change in the grid size, the maximum variation in the Nusselt number occurs at the vertical walls. In going from the 120x120 grid to the 240x240 grid the top and bottom wall Nusselt numbers vary by less than 1%. However, the vertical wall Nusselt numbers vary by almost 10%. This result indicates that the solution is still not grid independent for the finest grid computed in the present study. Kirkpatrick and Bohn (1986) used the average of the four-hot/cold wall temperatures as the bulk temperature. The wall to bulk temperature difference was used to evaluate the Nusselt numbers. For the HCCC configuration they found that the relationship between Nusselt number to Rayleigh number collapsed to a single correlation for all four walls, namely

$$Nu = 0.346Ra^{0.285} \quad (12)$$

Using the same definition for the Nusselt numbers, the correlation for all four walls at the finest grid is given in Table 2. The maximum error in the prediction of heat transfer occurs for the top wall (an over prediction of approximately 78%). Studies carried out for the heating from the side configuration (cf. Henkes; 1990) show that the heat transfer results for natural convection flows depend significantly on the turbulence model used as well as the near wall treatment. However, it is not the objective of the present paper to evaluate different turbulence models. Instead, the comparison exercise gives an estimate of the error in the heat transfer prediction given by the present model.

Grid	Left wall	Right wall	Top wall	Bottom wall
60x60	0.3660	0.3635	0.6221	0.2531
120x120	0.4284	0.4268	0.6181	0.2663
240x240	0.4736	0.4724	0.6168	0.2674

Table 2: Coefficient of the relationship between Nusselt number to Rayleigh number.

Case study: Discussion of results

The geometry for the case study is shown in Figure 1. A 60x60 non-uniform grid was used as a compromise between accuracy and computing time. For the unsteady calculations, a time step of 0.1 s was used until the temperature and velocity fields were almost converged in the fluid layer. The convergence was monitored through changes in the wall Nusselt numbers. Approximately 3000 time steps were required. The time step was then increased to 10 s, for monitoring changes in the moisture content and changes in temperature in the porous layer. Any further increase in the time step lead to divergence. Due to the very small number of internal iterations between two time iterations, (typically three to four internal iterations are required), computations for significantly large real times can be carried out in relatively short machine times. For the largest real time calculated in the present case study, 50 hours, a CPU time of around 5 hours was required on a Pentium II (350 MHz). However, increasing the time step is desirable for shorter computational times. The changes in the isotherms and moisture content of air are shown in Figures 5 and 6 respectively after 10, 30 and 50 hours. Changes in moisture content of the porous medium have not been shown here, because they were found to be insignificant in this period of time. The heat and moisture from the porous medium is driven towards the fluid layer through the central rising plume as seen in Figures 5 and 6. The thermal plume is expected to enhance the transport of heat, and hence, moisture from the porous medium. Thus the accurate prediction of heat transfer by the turbulence model is very important. Due to the heat transfer, the core of the porous medium becomes progressively cooler, as can be seen from Figure 5. Similarly, from Figure 6, one can see that the moisture content of the air in the porous medium decreases as time progresses. As the air gets cooler, its ability to hold moisture decreases, and this extra moisture is adsorbed by the hygroscopic porous medium. In case of grains this

phenomenon has important implications, as it leads to the growth of moulds in these regions which eventually destroy the grains. It was found that close to the sidewalls and in the region close to the central rising plume in the porous medium, the moisture content of the porous medium increases. This increase becomes significant as time progresses. It is evident from Figure 5 that these are regions of relative coolness in the porous medium.

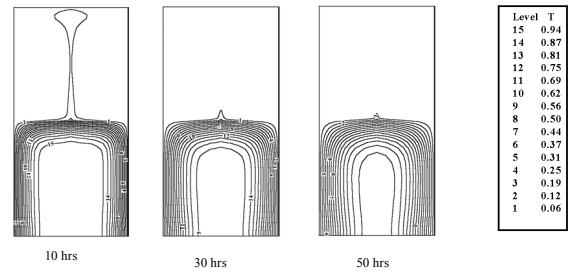


Figure 5: Change in isotherms for the case study

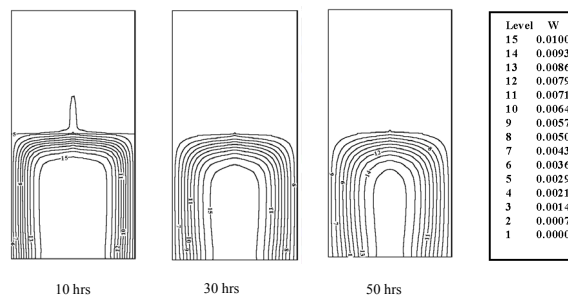


Figure 6: Change in air moisture content for the case study

CONCLUSION

A general procedure of simulating systems with a turbulent flow overlying a saturated hygroscopic porous medium has been presented. Emphasis has been placed on using this model for simulating moisture migration in stored agricultural products. Such a model is capable of predicting the moisture migration process more accurately by accounting for turbulence in the fluid layer. The level of sophistication of the turbulence model is limited by the comparatively large run times encountered to simulate such systems. The model needs to be validated further with realistic experimental data. The present model is capable of simulating flows only when turbulence in the porous medium can be considered to be negligible. However, this condition would not be true for porous media of high permeability. In order to overcome this limitation, a turbulence model for the porous medium needs to be incorporated into the existing model.

REFERENCES

- CHEN, L. and LI, Y., (1999), "Modelling high Rayleigh number natural convection flows in grain storage", *CSIRO Research Report*, BCE DOC. 99/0331 (M).
- CHEN, L., LI, Y. and THORPE, G.R., (1998), "High-Rayleigh-number natural convection in an enclosure containing a porous layer", *11th Int. Heat Transfer Conf.*, Seoul, Korea.
- HENKES, R.A.W.M., (1990), "Natural convection boundary layers", *Ph.D. Thesis, Delft Univ. Tech., The Netherlands*.
- HUNTER, A.J., (1987), "An isostere equation for some common seeds", *J. Agric. Eng. Res.*, **37**, 93-107.
- KIRKPATRICK, A.T. and BOHN, M., (1986), "An experimental investigation of mixed cavity natural convection in the high Rayleigh number regime", *Int. J. Heat and Mass Transfer*, **29**, 69-82.
- NEALE, G. and NADER, W., (1974), "Practical significance of Brinkman's extension of Darcy's law: Coupled parallel flows within a channel and a bounding porous medium", *Canadian J. Chem. Eng.*, **52**, 475-478.
- PATANKAR, S.V., (1980), "Numerical Heat Transfer and Fluid Flow", *Hemisphere Publishing Corporation, USA*.
- PRAKASH, M., MAHONEY, J., Li, Y., TURAN, Ö.F. and THORPE, G.R., (1999a), "Flow visualisation for an enclosed axi-symmetric impinging round jet with and without porous medium" (in preparation).
- PRAKASH, M., TURAN Ö.F. and THORPE G.R., (1999b), "Program Natcon: for the numerical solution of natural convection in a rectangular cavity", *Victoria Univ. Research Report*.
- PRAKASH, M., TURAN Ö.F. and THORPE G.R., (1999c), "Natural convection heat and mass transfer in hygroscopic porous media of low permeability", *Victoria Univ. Research Report*.
- SINGH, A.K., LEONARDI, E. and THORPE, G.R., (1993), "Three-dimensional natural convection in a confined fluid overlying a porous layer", *J. Heat Transfer*, **115**, 631-638.
- SONG, M. and VISKANTA, R., (1994), "Natural convection flow and heat transfer within a rectangular enclosure containing a vertical porous layer", *Int. J. Heat and Mass Transfer*, **37**, 2425-2438.
- SUTHERLAND, J.W., BANKS P.J. and GRIFFITHS, H.J., (1971), "Equilibrium heat and moisture transfer in air flow through grain", *J. Agric. Eng. Res.*, **16**, 368-386
- THORPE, G.R., MOORE, G.A. and SINGH, A.K., (1992), "Heat, mass and momentum transfer in three-dimensional bulks of stored grains", *Conf. on Eng. in Agric.*, Albury, NSW.